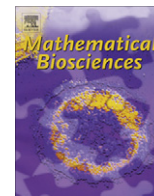


Contents lists available at ScienceDirect

Mathematical Biosciences

journal homepage: www.elsevier.com/locate/mbs

Describing the geographic spread of dengue disease by traveling waves[☆]

Norberto Aníbal Maidana^{*,1}, Hyun Mo Yang²

UNICAMP – IMECC/DMA, Caixa Postal 6065, CEP: 13083-970 Campinas, SP, Brazil

ARTICLE INFO

Article history:

Received 10 October 2007

Received in revised form 21 May 2008

Accepted 29 May 2008

Available online 12 June 2008

Keywords:

Dengue

Aedes aegypti

Traveling waves

Control

ABSTRACT

Dengue is a human disease transmitted by the mosquito *Aedes aegypti*. For this reason geographical regions infested by this mosquito species are under the risk of dengue outbreaks. In this work, we propose a mathematical model to study the spatial dissemination of dengue using a system of partial differential reaction–diffusion equations. With respect to the human and mosquito populations, we take into account their respective subclasses of infected and uninfected individuals. The dynamics of the mosquito population considers only two subpopulations: the winged form (mature female mosquitoes), and an aquatic population (comprising eggs, larvae and pupae). We disregard the long-distance movement by transportation facilities, for which reason the diffusion is considered restricted only to the winged form. The human population is considered homogeneously distributed in space, in order to describe localized dengue dissemination during a short period of epidemics. The cross-infection is modeled by the law of mass action. A threshold value as a function of the model's parameters is obtained, which determines the rate of dengue dissemination and the risk of dengue outbreaks. Assuming that an area was previously colonized by the mosquitoes, the rate of disease dissemination is determined as a function of the model's parameters. This rate of dissemination of dengue disease is determined by applying the traveling wave solutions to the corresponding system of partial differential equations.

© 2008 Elsevier Inc. All rights reserved.

1. Introduction

The dengue virus is transmitted by arthropods of the genus *Aedes*. The cosmopolitan mosquito, *Aedes aegypti* (Linn. Diptera: Culicidae), serves as the most important domestic vector of dengue and urban yellow fever. The dengue virus is prevalent in different parts of the world and its epidemiological cycle comprises a human host and a vector—the *Aedes aegypti* mosquito. Female *A. aegypti* mosquitoes interact closely with humans as they need to feed on human blood to fertilize their eggs, thus characterizing the urban feature of this epidemic. As the dengue virus is pathogenic for humans and capable of transmission in heavily populated areas, it can cause widespread and serious epidemics, appearing as a major public health problem in many tropical and subtropical regions of the world.

In Brazil, dengue disease is currently one of the main public health challenges and has shown an increase in the number of cases and in its geographical distribution over time. For instance, in 1998, 537,507 cases of dengue were reported in 24 states, with

98 cases of hemorrhagic dengue in 9 states. In the same year, in the state of São Paulo, 10,629 cases of dengue disease occurred in 102 municipalities, overcoming increased efforts expended by the public health authorities on the control of *A. aegypti*. In 2000, there were 230,910 cases of dengue, with 51 cases of hemorrhagic dengue in 8 states [1]. The re-emergence of dengue transmission in Brazil could be due to deteriorating socioeconomic conditions, climatic changes caused by global warming (e.g.: the “El Niño” phenomenon), discontinuous sanitary activities, among other factors.

With respect to dengue disease, the dengue virus has four different serotypes with low cross-immunity among them, which can result in secondary infections after an infection with one serotype has occurred. It is known that an individual infected with one serotype can be infected with another serotype six months after the first exposure, but there is no evidence of reinfection with the same serotype. The dengue virus of all four serotypes cause three distinct syndromes: classic dengue fever, dengue hemorrhagic fever (DHF) and dengue shock syndrome. Although caused by the same virus, dengue and dengue hemorrhagic fever are pathogenically, clinically and epidemiologically distinct.

There are many mathematical models dealing with the transmission of dengue disease restricted only to one serotype. For instance, Esteva and Vargas proposed a model where they determined the threshold conditions to assess vector control [2], analyzing the effects of vertical transmission on the overall dengue epidemics [3]. However, mathematical modeling regarding

[☆] Grant from FAPESP (Projeto Temático).

* Corresponding author. Tel.: +55 19 37812147.

E-mail addresses: nmaidana@ime.unicamp.br (N.A. Maidana), hyunyang@ime.unicamp.br (H.M. Yang).

¹ Fellowship from FAPESP (Postdoctoral fellowship).

² Fellowship from CNPq.

transmission of two different dengue serotypes is not an easy task. Esteva and Vargas [4] obtained the basic reproduction numbers regarding the first and secondary infections from a dengue transmission model with two different serotypes. Derouich and Bou-tayeb [5] proposed a model for studying the dynamics of two serotypes of dengue epidemic. They considered that one of the human subpopulations is comprised of individuals removed from the first infection (e.g.: serotype 1) which were exposed to secondary infection (with a different serotype). Nevertheless, the dynamics of this subpopulation follows a decreasing trajectory, in which the initial input of primarily infected individuals is exhausted. A spatially heterogeneous model was proposed by Cummings et al. [6]. They analyzed the occurrence of spatially distributed dengue hemorrhagic fever in Thailand via traveling waves by applying the empirical mode decomposition (EMD) method. This method was applied taking human movement into account, which is relevant in the DHF patterns in Thailand. Tran and Raffy [7] considered a spatial dengue model, but they did not consider human movement because they were interested in local dengue dissemination across small regions.

In this paper we propose a spatial dissemination of one serotype of the dengue virus, assuming that only adult mosquitoes are allowed diffusive movement. In addition to this winged phase, we attribute only one aquatic phase to the mosquito life cycle, which encompasses eggs, larvae and pupae. The fast spread of dengue disease can be explained by intense human movements [6]. Our main task is to determine the speed of dengue dissemination following the invasion and colonization by *A. aegypti* mosquitoes in the state of São Paulo, Brazil. First, from a simple model where only the mosquito population is allowed movements (diffusion and advection), we obtain the equation for the speed of dengue disease dissemination. This model should be a description of dengue dissemination from vicinity to vicinity originated from a single infectious individual introduced in a region; hence the rate of dengue dissemination obtained this way can be understood as a result of the movements by the mosquito population. In addition, by taking the movements of humans into account, we show numerically how the speed of dengue disease dissemination increases.

The state of São Paulo can be approximated roughly by a parallelogram with a 690-km dimension in the Northwest-Southeast direction and 440 km in the Northeast-Southwest direction. The state of São Paulo is located in a subtropical region, where summer is hot and rainy and where *A. aegypti* was reintroduced in 1985 from the North border, continuously advancing southwards [8]. The epidemics of dengue serotype 1 was first observed in 1987, but its annual occurrence systematically started in 1990; however, in 1996, dengue serotype 2 was introduced, and, in 2001, serotype 3 was detected in the state of São Paulo [1]. The numbers of cases of dengue from 1995 until 2006 were, respectively, 6,048, 7,104, 2,040, 10,630, 15,082, 3,532, 51,668, 39,179, 20,390, 3,049, 5,433 and 50,022 [9]. In 2007, the number of cases was 64,661 up to September.

In this paper we deal with the invasion and colonization of *A. aegypti* mosquitoes followed by the establishment of the dengue epidemics. In Section 2, we develop a model for dengue transmission allowing movements only to mosquitoes, which is analyzed in Section 3. In Section 4, we obtain the traveling wave solutions. In Section 5, we also consider the movements of humans, and the traveling wave solutions are obtained numerically. Finally, conclusions are stated in Section 6.

2. Model for the transmission of dengue disease

Dengue disease is a vector-borne viral infection transmitted among humans by mosquito bite during the blood meal. We pro-

pose a model by taking into account the human and the mosquito populations.

Our aim is to describe the occurrence of dengue infection in a region infested by mosquitoes, but free of disease. Another feature of the model is the restriction of the movements only to the mosquito population in the spatial dengue dissemination, whereby we disregard nonlocal effects, that is, the spread of the disease due to intense movements of human individuals.

The human population is divided into susceptible, infected and removed (or immune) individuals. The spatial densities at time t are denoted by $\bar{H}(x, t)$, $\bar{I}(x, t)$ and $\bar{R}(x, t)$, respectively. The human population is under a constant per capita mortality rate $\bar{\mu}_H$. The total population is designated by $\bar{N}(x, t) = \bar{H}(x, t) + \bar{I}(x, t) + \bar{R}(x, t)$.

With respect to the mosquito population, we consider the winged and aquatic (comprising eggs, larvae and pupae) subpopulations, whose spatial densities are denoted by $\bar{M}(x, t)$ and $\bar{A}(x, t)$, respectively [10]. The per capita oviposition rate is $r(1 - \frac{\bar{A}}{k_2})$, where the intrinsic oviposition rate is denoted by r and k_2 is the carrying capacity (available amount of breeding sites) regarding the aquatic form. The carrying capacity regarding the winged form is denoted by k_1 , taking into account the fact that mosquitoes are not able to survive at high altitudes. The per capita rate of maturation from the aquatic form to the winged one is denoted by $\bar{\gamma}$. The immature (aquatic form) population of mosquitoes is under the per capita mortality rate $\bar{\mu}_2$, and the per capita mortality rate of the winged form is $\bar{\mu}_1$. With respect to the winged form, the susceptible and the infected classes are designated by $\bar{M}_S(x, t)$ and $\bar{M}_I(x, t)$, respectively, and the total population is $\bar{M}(x, t) = \bar{M}_S(x, t) + \bar{M}_I(x, t)$.

We assume the law of mass action to describe the transmission of dengue infection among humans and mosquitoes. The constant transmission coefficient $\bar{\beta}_1$, which measures the rate of effective contact between uninfected mosquitoes and infected humans, is the rate at which susceptible mosquitoes are infected when they bite infectious humans. The other is $\bar{\beta}_2$, which measures the rate of effective contact between uninfected humans and infected mosquitoes.

These transmission coefficients depend on the average biting rate b , the average transmission probability β_V from human to vector, and β_H , from vector to human, as in [2,3]. These parameters are normalized by the constant human population \bar{N}_0 , because in this model we consider the ‘pseudo’ law of mass action regarding the mosquito population. Hence, we have $\bar{\beta}_1 = b\beta_V/\bar{N}_0$ and $\bar{\beta}_2 = b\beta_H/\bar{N}_0$. We consider $b = 0.5$ (one bite every two days), $\beta_V = 1$ and $\beta_H = 0.75$ as in [2,3]. The human population is assumed to be $\bar{N}_0 = 150$ per km^2 , considering the population and the territory of the state of São Paulo.

Considering the natural history of infection, the infected humans are transferred at a rate $\bar{\sigma}$ to the removed (or immune) class, remaining in this class forever. Hence, we assume lifelong immunity among humans, but we do not consider immunity among mosquitoes. Finally, we recall our assumption about the geographical dispersal of *A. aegypti*, while humans are assumed to be homogeneously distributed in space. Hence, both infected and uninfected classes of mosquitoes are under diffusion by wings and by winds, described by the diffusion parameter \bar{D} and advection \bar{v} , respectively.

The model, which governs the spatial and temporal evolution of the disease, is the following:

$$\frac{\partial \bar{M}_S}{\partial t} = \bar{D} \frac{\partial^2 \bar{M}_S}{\partial x^2} - \bar{v} \frac{\partial \bar{M}_S}{\partial x} + \bar{\gamma} \bar{A} \left(1 - \frac{\bar{M}}{k_1}\right) - \bar{\mu}_1 \bar{M}_S - \bar{\beta}_1 \bar{M}_S \bar{I} \quad (1)$$

$$\frac{\partial \bar{M}_I}{\partial t} = \bar{D} \frac{\partial^2 \bar{M}_I}{\partial x^2} - \bar{v} \frac{\partial \bar{M}_I}{\partial x} - \bar{\mu}_1 \bar{M}_I + \bar{\beta}_1 \bar{M}_S \bar{I} \quad (2)$$

$$\frac{\partial \bar{A}}{\partial t} = r \left(1 - \frac{\bar{A}}{k_2}\right) \bar{M} - \bar{\mu}_2 \bar{A} - \bar{\gamma} \bar{A} \quad (3)$$

$$\frac{\partial \bar{H}}{\partial t} = \bar{\mu}_H \bar{N} - \bar{\mu}_H \bar{H} - \bar{\beta}_2 \bar{H} \bar{M}_I \tag{4}$$

$$\frac{\partial \bar{I}}{\partial t} = \bar{\beta}_2 \bar{H} \bar{M}_I - \bar{\sigma} \bar{I} - \bar{\mu}_H \bar{I} \tag{5}$$

$$\frac{\partial \bar{R}}{\partial t} = \bar{\sigma} \bar{I} - \bar{\mu}_H \bar{R}, \tag{6}$$

where the non-negative parameters and variables were previously defined for the model. The transmission coefficients $\bar{\beta}_1$ and $\bar{\beta}_2$ are per capita quantities, since we are not dealing with fractions of individuals.

Let us initially analyze the system of Eqs. (1)–(6) disregarding dengue transmission. Adding up the last three equations of the system, we obtain the density of the human population \bar{N} , $\bar{N} = \bar{H} + \bar{I} + \bar{R}$, which is given by:

$$\frac{\partial \bar{N}}{\partial t} = \frac{\partial \bar{H}}{\partial t} + \frac{\partial \bar{I}}{\partial t} + \frac{\partial \bar{R}}{\partial t} = 0,$$

which yields a constant population due to the fact that we have assumed that the overall input (comprising natality and immigrations) is balanced by overall mortality (encompassing mortality and emigration) $\bar{\mu}_H \bar{N}$, and we are not taking into account the disease-induced mortality. Therefore $\bar{N} = \bar{N}_0$ is constant.

Now, adding up the first two equations of the system, with $\bar{M}(x, t) = \bar{M}_S(x, t) + \bar{M}_I(x, t)$, we have the equations for the dispersal of the mosquito population:

$$\frac{\partial \bar{M}}{\partial t} = \bar{D} \frac{\partial^2 \bar{M}}{\partial x^2} - \bar{v} \frac{\partial \bar{M}}{\partial x} + \bar{\gamma} \bar{A} \left(1 - \frac{\bar{M}}{k_1} \right) - \bar{\mu}_1 \bar{M}$$

$$\frac{\partial \bar{A}}{\partial t} = r \left(1 - \frac{\bar{A}}{k_2} \right) \bar{M} - \bar{\mu}_2 \bar{A} - \bar{\gamma} \bar{A}.$$

This is the system of equations analyzed in [10] for the *A. aegypti* dispersal dynamics in the absence of dengue disease.

Let us introduce the non-dimensional parameters to the system of equations Eqs. (1)–(6). The winged and aquatic phases of the mosquito population are scaled by the respective carrying capacities and the human population is scaled by the total population $\bar{N}_0 = \bar{N}$; the time is scaled with respect to the oviposition rate r , the spatial scaling is given by the square root of the quotient between mosquito diffusion and the oviposition rate, $\sqrt{\frac{D}{r}}$. Therefore, the non-dimensional parameters are:

$$M_S = \frac{\bar{M}_S}{k_1}, \quad M_I = \frac{\bar{M}_I}{k_1}, \quad A = \frac{\bar{A}}{k_2}, \quad H = \frac{\bar{H}}{\bar{N}}, \quad I = \frac{\bar{I}}{\bar{N}}, \quad R = \frac{\bar{R}}{\bar{N}} \tag{7}$$

$$k = \frac{k_1}{k_2}, \quad v = \frac{\bar{v}}{r} \left(\frac{r}{D} \right)^{1/2}, \quad \gamma = \frac{\bar{\gamma}}{r}, \quad \mu_1 = \frac{\bar{\mu}_1}{r}, \quad \mu_2 = \frac{\bar{\mu}_2}{r} \tag{8}$$

$$\beta_1 = \frac{\bar{\beta}_1 \bar{N}}{r}, \quad \beta_2 = \frac{\bar{\beta}_2 k_1}{r}, \quad \mu_H = \frac{\bar{\mu}_H}{r}, \quad \sigma = \frac{\bar{\sigma}}{r}. \tag{9}$$

Since $R = 1 - H - I$, we can omit the equation for R . Therefore, the corresponding non-dimensional system is:

$$\frac{\partial M_S}{\partial t} = \frac{\partial^2 M_S}{\partial x^2} - v \frac{\partial M_S}{\partial x} + \frac{\gamma}{k} A(1 - M) - \mu_1 M_S - \beta_1 M_S I \tag{10}$$

$$\frac{\partial M_I}{\partial t} = \frac{\partial^2 M_I}{\partial x^2} - v \frac{\partial M_I}{\partial x} - \mu_1 M_I + \beta_1 M_S I \tag{11}$$

$$\frac{\partial A}{\partial t} = k(1 - A)M - \mu_2 A - \gamma A \tag{12}$$

$$\frac{\partial H}{\partial t} = \mu_H - \mu_H H - \beta_2 H M_I \tag{13}$$

$$\frac{\partial I}{\partial t} = \beta_2 H M_I - \sigma I - \mu_H I. \tag{14}$$

Note that the human population is normalized and the recovered individuals are decoupled from the system.

3. Analysis of the spatially homogeneous dynamics

Let us analyze the spatially homogeneous dynamics, assuming that the mosquito population has reached spatial homogeneity:

$$\frac{dM_S}{dt} = \frac{\gamma}{k} A(1 - M) - \mu_1 M_S - \beta_1 M_S I \tag{15}$$

$$\frac{dM_I}{dt} = -\mu_1 M_I + \beta_1 M_S I \tag{16}$$

$$\frac{dA}{dt} = k(1 - A)M - \mu_2 A - \gamma A \tag{17}$$

$$\frac{dH}{dt} = \mu_H - \mu_H H - \beta_2 H M_I \tag{18}$$

$$\frac{dI}{dt} = \beta_2 H M_I - \sigma I - \mu_H I. \tag{19}$$

The system of Eqs. (15)–(19) has three steady states. The steady state with only the human population is given by

$$E_0 = (M_S^0, M_I^0, A^0, H^0, I^0) = (0, 0, 0, 1, 0).$$

This equilibrium point represents an area free of mosquitoes, which can be invaded and colonized by the mosquito population if appropriate traveling front waves are achieved [10].

The second equilibrium represents regions where mosquitoes are well established, but free of dengue disease:

$$E_1 = (M_S^1, M_I^1, A^1, H^1, I^1) = (m^*, 0, a^*, 1, 0),$$

where

$$a^* = \frac{k(1 - Q_0^{-1})}{k + \mu_2 + \gamma} \quad \text{and} \quad m^* = \frac{\gamma(1 - Q_0^{-1})}{\mu_1 k + \gamma}.$$

The biological feasibility for the existence of the mosquito population implies that:

$$Q_0 > 1, \tag{20}$$

where the ecological parameter Q_0 is

$$Q_0 = \frac{\gamma}{\mu_1(\gamma + \mu_2)}.$$

This condition can be written in terms of dimensional parameters, resulting in the basic offspring number \bar{Q}_0 ,

$$\bar{Q}_0 = \frac{\bar{\gamma}}{\bar{\gamma} + \bar{\mu}_2} \times \frac{r}{\bar{\mu}_1}.$$

This number gives the average number of female mosquitoes produced by one fertile mosquito. Indeed, the first term $(\frac{\bar{\gamma}}{\bar{\gamma} + \bar{\mu}_2})$ is the probability for a viable egg laid by the female mosquito to survive the entire aquatic phase and emerge as a female mosquito, and the second term $(\frac{r}{\bar{\mu}_1})$ is the average number of viable eggs laid by the emerging female mosquito during its entire lifespan. Note that if the average number of female mosquitoes produced by one mosquito is higher than one ($Q_0 > 1$), then the mosquito population persists in the colonized region.

The third steady state, which corresponds to the disease at an endemic level, is given by:

$$E^* = (M_S^*, M_I^*, A^*, H^*, I^*),$$

where the coordinates are

$$M_S^* = m^* - M_I^*, \quad M_I^* = \frac{(1 - H^*) \mu_H}{\beta_2 H^*}, \quad A^* = a^*,$$

$$H^* = 1 - \frac{(\mu_H + \sigma) I^*}{\mu_H}, \quad I^* = \frac{\mu_1 \mu_H (R_0 - 1)}{(\beta_1 \mu_H + \beta_1 \beta_2 m^*)},$$

where the basic reproduction number R_0 is given by

$$R_0 = \frac{\beta_1 \beta_2 m^*}{\mu_1 (\mu_H + \sigma)}$$

The equilibrium E^* is biologically feasible if two conditions are satisfied: $a^* > 0$ and $I^* > 0$. The first condition is satisfied if $Q_0 > 1$, while the second condition is verified if $R_0 > 1$.

The stability of the equilibrium points is determined by Q_0 and R_0 . We have the following results:

Theorem 3.1. *The equilibrium point $E_0 = (0, 0, 0, 1, 0)$ is locally asymptotically stable if and only if $Q_0 < 1$.*

Proof. See Appendix A. □

This result is due to the fact that $Q_0 < 1$ is the condition for the nonexistence of the mosquito population. This represents the steady state where mosquitoes are led to extinction and the disease fades out.

Theorem 3.2. *The equilibrium point $E_1 = (m^*, 0, a^*, 1, 0)$ is locally asymptotically stable if and only if $Q_0 > 1$ and $R_0 < 1$.*

Proof. See Appendix A. □

This means that the mosquito and human populations coexist without disease. If $Q_0 > 1$ and $R_0 > 1$, then $E^* = (M_s^*, M_i^*, A^*, H^*, I^*)$ is locally asymptotically stable. This means that the conditions for the existence of mosquitoes and the disease at an endemic level must be satisfied. The study of this fact is done numerically, because the characteristic polynomial of the Jacobian matrix is a fifth-degree polynomial.

The basic reproduction number R_0 , in terms of dimensional parameters, is:

$$\bar{R}_0 = \frac{\bar{\beta}_1 \bar{N}}{\bar{\mu}_1} \times \frac{\bar{\beta}_2 k_1 m^*}{\bar{\mu}_H + \bar{\sigma}}$$

This epidemiological parameter measures the average number of secondary infections among mosquitoes produced by one infectious mosquito in completely susceptible populations of humans and mosquitoes. Note that $\bar{\beta}_1 \bar{N}$ is the total transmission coefficient among mosquitoes, and $\bar{\beta}_2 k_1 m^*$ is the total quantity of infection among humans. Therefore, the outbreaks of epidemics occur if $R_0 > 1$, but this condition must be achieved by the existence of mosquitoes, which is $Q_0 > 1$ in order to have $m^* > 0$.

The basic reproduction number is a threshold value, and also determines the endemic level of the disease. The estimation of this parameter is important for control strategies. For the dimensional parameters, corresponding to an average temperature of 30 °C (for other temperatures, see Table 5 below) listed in Tables 1 and 2, the basic reproduction number is $R_0 = 7.29$. By changing only the density of human population to $\bar{N}_0 = 100$ per km², the basic reproduction number decreases to $R_0 = 4.86$. In both cases, the outbreak of an epidemics can occur and propagate in a region that was previously free of disease.

Table 1
Parameters regarding *A. aegypti* invasion

Parameter	Symbol	Value
Diffusion coefficient	\bar{D}	$1,25 \times 10^{-2}$ km ² /day
Advection coefficient	v	5×10^{-2} km/day
Period of time in aquatic form	$\bar{\gamma}^{-1}$	5 day
Oviposition rate	\bar{r}	10 day ⁻¹
Carrying capacity—winged form	k_1	25 individuals/km ²
Carrying capacity—aquatic form	k_2	100 individuals/km ²
Survival time in winged phase	$\bar{\mu}_1^{-1}$	35 days
Survival time in aquatic phase	$\bar{\mu}_2^{-1}$	18 days

The entomological parameters are those corresponding to 30 °C, Takahashi et al. [10], Yang et al. [11] and Harrington et al. [12].

Table 2
Parameters regarding dengue disease transmission, Esteva and Vargas [2,3], Veronesi [13]

Parameter	Symbol	Value
Per-capita contact rate—infection among mosquitoes	$\bar{\beta}_1$	0.0033 km ² /day
Per-capita contact rate—infection among humans	$\bar{\beta}_2$	0.0025 km ² /day
Life expectancy in humans	$\bar{\mu}_H^{-1}$	60 years
Infectious period	$\bar{\sigma}^{-1}$	7 days
Constant number of humans	\bar{N}	150 individuals/km ²

In the next section, we study the possible existence of the traveling wave solutions connecting the steady states E_0 with E_1 and E_1 with E^* . The first connection concerns the mosquitoes colonizing some region and, then, the disease begins to propagate in this region if the second connection is allowed.

4. Traveling wave solutions

We study two situations. The first scenario corresponds to the human population free of mosquitoes; then an invasion of mosquitoes occurs, which was studied in [10]. The second situation considers that the mosquito population is well established among humans but that dengue disease is absent. In this scenario, we analyze the dissemination of dengue disease when a small number of infective individuals (humans and/or mosquitoes) is introduced into this community. Hence, we seek the existence of traveling wave solutions connecting E_0 with E_1 and E_1 with E^* , respectively, to describe the first and the second scenarios.

In order to obtain the traveling wave solutions, we must determine the minimum speed of these waves [14,15], because it is stable and represents the observable trajectory of the dynamics system [16,17]. The traveling wave solutions, when they exist, must be represented by:

$$(\tilde{m}_s(x, t), \tilde{m}_i(x, t), \tilde{a}(x, t), \tilde{h}(x, t), \tilde{i}(x, t)) = (m_s(z), m_i(z), a(z), h(z), i(z)),$$

where $z = x + ct$, and c is a constant speed [14]. By applying this change of variable to the system of Eqs. (10)–(14), we obtain the corresponding non-dimensional system of the first-order ordinary differential equations:

$$\frac{dm_s}{dz} = u, \tag{21}$$

$$\frac{du}{dz} = (c + v)u - \frac{\gamma}{k}(1 - m)a + \mu_1 m_s + \beta_1 m_s i \tag{22}$$

$$\frac{dm_i}{dz} = v, \tag{23}$$

$$\frac{dv}{dz} = (c + v)v + \mu_1 m_i - \beta_1 m_s i \tag{24}$$

$$\frac{da}{dz} = (1/c)(k(1 - a)m - \mu_2 a - \gamma a) \tag{25}$$

$$\frac{dh}{dz} = (1/c)(\mu_H n - \mu_H h - \beta_2 h m_i) \tag{26}$$

$$\frac{di}{dz} = (1/c)(\beta_2 h m_i - \sigma i - \mu_H i). \tag{27}$$

Let us apply this system of equations to describe the mosquito invasion and the spread of dengue.

4.1. *A. aegypti* invasion

Let us first assess, in the three-dimensional submanifold

$$\tilde{M} = \{(m_s, u, m_i, v, a, h, i) : m_i = 0, v = 0, h = 1, i = 0\},$$

the existence of traveling wave solutions connecting E_0 with E_1 , which represents the mosquito invasion in regions previously free of mosquitoes. The traveling wave solutions, if they exist, must satisfy the boundary conditions:

$$(m_s(-\infty), u(-\infty), m_i(-\infty), v(-\infty), a(-\infty), h(-\infty), i(-\infty)) = \hat{E}_0 = (0, 0, 0, 0, 0, 1, 0)$$

and

$$(m_s(\infty), u(\infty), m_i(\infty), v(\infty), a(\infty), h(\infty), i(\infty)) = \hat{E}_1 = (m^*, 0, 0, 0, a^*, 1, 0).$$

The zeros in both equilibrium points \hat{E}_0 and \hat{E}_1 deserve some comment. Considering the submanifold \bar{M} , the unique zero in the second equilibrium point \hat{E}_1 corresponds to the derivative of m_s . However, the first equilibrium point \hat{E}_0 has two more zeros corresponding to mosquitoes in the adult and aquatic phases, which must not be negative densities. Due to this constraint, we impose that the linear system solutions must not oscillate, i.e., the eigenvalues corresponding to \hat{E}_0 must assume real values. The stability of the equilibrium point \hat{E}_0 with respect to the linear system of Eqs. (21)–(27) is now assessed. The corresponding eigenvalues are:

$$\lambda_1 = -\frac{\mu_H}{c}, \quad \lambda_2 = -\frac{\mu_H + \sigma}{c}, \quad \lambda_{3,4} = \frac{1}{2} \left[c + v \pm \sqrt{(c + v)^2 + 4\mu_1} \right],$$

which are real, plus the roots of the third-degree polynomial:

$$P(\lambda) = \lambda^3 + \left[-(c + v) + \frac{(\mu_2 + \gamma)}{c} \right] \lambda^2 - \left[\mu_1 + (c + v) \frac{(\mu_2 + \gamma)}{c} \right] \lambda + \frac{\mu_1(\gamma + \mu_2)(Q_0 - 1)}{c}. \tag{28}$$

We are dealing with the biological system, whose variables describe the densities of individuals. Hence, all solutions must be positively defined in order to avoid the dynamic trajectories oscillations around the trivial equilibrium point. This constraint is obeyed if all the eigenvalues assume real values. This condition determines the equation for the speed of invasion, when c satisfies $P(\lambda_+) = 0$, where λ_+ is the minimum extremum of polynomial (28). See Appendix B for more details. Polynomial (28), which depends on the model’s parameters, was used in [10] to assess the control strategies in order to avoid mosquito invasion.

Using the set of entomological parameters corresponding to 30 °C given in Table 1, and disregarding the advection movement, the speed of invasion was determined to be $\bar{c} = 75.46$ km/year, which was obtained by solving equation $P(\lambda_+) = 0$, where the polynomial is given by (28). Taking into account the temperature-dependent entomological parameters [11], the calculations of the theoretical front wave speeds for different temperatures are given in Table 3. If we consider the advection movement, $\bar{v} = 18.25$ km/year, [10], we obtain $\bar{c} = 89.67$ km/year for 30 °C.

Let us now study the invasion of mosquito *A. aegypti* in the state of São Paulo, Brazil, by taking into account the maps of *A. aegypti*

Table 3
Entomological parameters regarding *A. aegypti* for three different temperatures, Yang et al. [11]

(°C)	r (day ⁻¹)	$\bar{\gamma}^{-1}$ (day)	$\bar{\mu}_1^{-1}$ (day)	$\bar{\mu}_2^{-1}$ (day)	Invasion speed (km/year)
15	1.52	52.63	26.3	50	22
20	3.97	13.51	27	34.5	45.6
25	6.95	8.26	29.4	17.2	60.14
30	10	5	35	18	75.46

By considering these values we calculated the theoretical front wave speed, disregarding the advection movement ($\bar{v} = 0$).

colonization, temperature and rainfall found in [8]. Roughly, the shape of the state of São Paulo can be approximated as a parallelogram. On the southern border, we have the Atlantic Ocean, and on the northern border, we have the state of Mato Grosso. On the east side, we have two states: Rio de Janeiro, occupying a small part in the extreme of the southern border, and the state of Minas Gerais, occupying almost all of the eastern border. On the western border, we have the state of Paraná.

We briefly describe the invasion of *A. aegypti* in the state of São Paulo. *A. aegypti* invasion initiated in the state of Mato Grosso and moved southwards to the Atlantic Ocean. Table 4 shows the distance traveled by the front wave of invasion for different years, with an average speed of 46.55 km/years during the time of observation 1985–1994. The northern region of the state of São Paulo is characterized by an annual mean temperature above 18 °C and an annual mean rainfall less than 1,400 mm [8]. The central and southern regions of the state of São Paulo present annual mean temperature and rainfall of, respectively, 17 °C and 1500 mm [8].

The invasion of *A. aegypti* began in the state of Mato Grosso, on the northern border of the state of São Paulo. The northern borders of the state of São Paulo are characterized by favorable conditions (high temperature and humidity), for which we observed a quick speed of invasion during the first six years, with the maximum speed occurring in the year 1990–1991, that is, 78.85 km/year. The central and southern regions of the state of São Paulo are characterized by less favorable conditions, and the speed of invasion of mosquitoes diminished by half during the last three years, with the minimum speed of the front wave of *A. aegypti* in 1992–1993, that is, 19.71 km/year. In 1994, the year of the last record provided in [8], the mosquito invasion occurred around 200 km far from the southern border, the Atlantic Ocean. The observed speeds of the mosquito invasion seem to indicate that abundance of rain should not be a favorable condition for the establishment of *A. aegypti*. However, the temperature plays a major role in the spreading of the mosquito.

We compare the observed average speed of *A. aegypti* invasion throughout nine years, 46.55 km/years, with the theoretical speed of front wave given in Table 3. The estimated speed of invasion can be matched to the theoretical speed of 45.6 km/year corresponding to a temperature of 20 °C. Notice that for the temperature between 15 and 30 °C, the theoretical wave speed varies from 22 to 75.46 km/year. Both lower and upper bounds of theoretical speeds of the front waves are very close to the minimum and maximum speeds of invasion observed in the state of São Paulo.

4.2. Dengue dissemination

Let us suppose that *A. aegypti* successfully colonized a region, for instance, the state of São Paulo. Our task is to assess the dissemination of dengue disease, determining the speed of the front wave of the disease. As we have previously pointed out, we are allowing movements only for the vector population. The reason is to determine the minimum speed of dengue dissemination, which can be

Table 4
Displacement of the front wave of *A. aegypti* mosquitoes in the state of São Paulo according to the time of invasion

Year	Mosquito dispersal (km)
1985–1986	49.28
1986–1987	64.06
1987–1988	34.5
1988–1989	64.06
1989–1990	54.2
1990–1991	78.85
1991–1992	29.67
1992–1993	19.71
1993–1994	24.64

understood as the contribution of vector movements to the spreading of dengue disease. This knowledge can help health authorities to mark bounds of the region where interventions must be applied against mosquitoes as soon as an infectious individual is detected.

Now we search traveling wave solutions connecting \hat{E}_1 with \hat{E}^* . By doing this we focus on the scenario where dengue disease is emerging (or re-emerging) in regions that were previously free of this disease. This means that the traveling wave solutions must link the boundary conditions:

$$(m_s(-\infty), u(-\infty), m_i(-\infty), v(-\infty), a(-\infty), h(-\infty), i(-\infty)) = \hat{E}_1 = (m^*, 0, 0, 0, a^*, 1, 0)$$

and

$$(m_s(\infty), u(\infty), m_i(\infty), v(\infty), a(\infty), h(\infty), i(\infty)) = \hat{E}^* = (M_s^*, 0, M_i^*, 0, A^*, H^*, I^*).$$

Again, the zeros in both equilibrium points need some explanations. The two zeros in the equilibrium point \hat{E}^* do not matter, because they correspond to the derivatives of the subpopulation of mosquitoes m_s and m_i , and oscillations around this equilibrium point do not result in negative density values. However, the equilibrium point \hat{E}_1 presents two more zeros than \hat{E}^* in the seven-dimensional manifold, which correspond to infectious subpopulations regarding mosquitoes (m_i) and humans (i). In order to assign positive densities to both infectious subpopulations, the solutions with respect to the linear system must not oscillate around zeros. In other words, the eigenvalues corresponding to \hat{E}_1 must assume real values. We stress the fact that the remaining two zeros regard derivatives, similar to \hat{E}^* .

Let us analyze the stability of the equilibrium point \hat{E}_1 with respect to the linear system of Eqs. (21)–(27). The eigenvalues are:

$$\lambda_1 = -\frac{\mu_H}{c},$$

plus the roots of two third-degree polynomials:

$$P_1(\lambda) = \lambda^3 + \left[-(c + v) + \frac{(\mu_H + \sigma)}{c}\right]\lambda^2 - \left[\mu_1 + (c + v)\frac{(\mu_H + \sigma)}{c}\right]\lambda + \frac{\mu_1(\mu_H + \sigma)(R_0 - 1)}{c} \quad (29)$$

and

$$P_2(\lambda) = \lambda^3 + \left[-(c + v) + \frac{\gamma + \mu_2 + km^*}{c}\right]\lambda^2 + \left[-(c + v)\frac{(\gamma + km^* + \mu_2)}{c} - \left(\frac{a^*\gamma + k\mu_1}{k}\right)\right]\lambda - \frac{\mu_1(\gamma + \mu_2)(Q_0 - 1)}{c}.$$

We use the same analysis performed in the previous subsection with respect to polynomials $P_1(\lambda)$ and $P_2(\lambda)$. We now avoid oscillations around the equilibrium point \hat{E}_1 , that is, m_i and i must not assume negative values. This is attained when all eigenvalues of $P_1(\lambda)$ and $P_2(\lambda)$ assume real values.

First, when the condition $Q_0 > 1$ is satisfied, we have $a^* > 0$ and $m^* > 0$, and we can show that all roots of polynomial $P_2(\lambda)$ are real (see Appendix B). Hence, the eigenvalues of polynomial $P_1(\lambda)$ allow obtaining minimum traveling wave speed of dengue dissemination, which is denoted by c_{min} .

The condition $R_0 > 1$ implies that $P_1(0) > 0$; additionally, we have:

$$\lim_{\lambda \rightarrow \pm\infty} P_1(\lambda) = \pm\infty, \quad \left. \frac{dP_1(\lambda)}{d\lambda} \right|_{\lambda=0} = -\left[\mu_1 + (c + v)\frac{(\mu_H + \sigma)}{c}\right] < 0.$$

Therefore, $P_1(\lambda)$ has always one negative real root. Moreover, the extreme of $P_1(\lambda)$ is

$$\lambda_{\pm} = \frac{1}{3} \left\{ -\left[-(c + v) + \frac{(\mu_H + \sigma)}{c}\right] \pm \sqrt{\left[-(c + v) + \frac{(\mu_H + \sigma)}{c}\right]^2 + 3\left[\mu_1 + (c + v)\frac{(\mu_H + \sigma)}{c}\right]} \right\},$$

where $\lambda_- < 0$ is the local maximum with $P_1(\lambda_-) > 0$, and $\lambda_+ > 0$ is the local minimum. We now impose that $P_1(\lambda_+)$ must assume at most zero value, that is, $P_1(\lambda_+) \leq 0$, in order to yield real-valued roots. Then, the double positive real root, which comes from $P_1(\lambda_+) = 0$, determines c_{min} (see Fig. 1). For $c < c_{min}$ there are complex solutions for $P_1(\lambda)$, and for $c > c_{min}$, two different positive real roots. Therefore, the equation $P_1(\lambda_+) = 0$ permits us to calculate c_{min} as a function of the parameters.

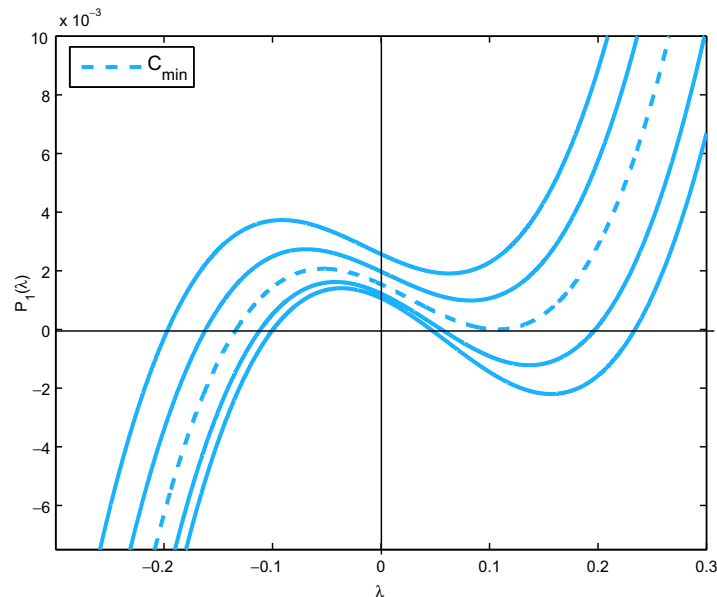


Fig. 1. Graph of the polynomial $P_1(\lambda)$ for the parameters corresponding to those listed in Tables 1 and 2, setting $v = 0$. The curves correspond to the values $c = 0.24$, $c = 0.21$, which have three real roots, $c_{min} = 0.167$ with double root, and $c = 0.13$ and $c = 0.1$, which have only one real root.

The non-dimensional speed, for the non-dimensional parameters corresponding to those listed in Tables 1 and 2, setting $v = 0$, is $c_{\min} = 0.167$. In the dimensional parameters this rate of dissemination of dengue disease is 0.06 km/day, i.e., 21.5 km/year.

In Fig. 2, the traveling waves corresponding to the system (21)–(27) are shown for the subpopulations of infected and uninfected humans, and for infected and uninfected mosquitoes. The cyclic front waves of the disease can be observed in Fig. 3(a) for infected subpopulations and in Fig. 3(b) for uninfected subpopulations.

Now we study the variation of the wave speed as a function of the model's parameters to assess the effects of control strategies.

Fig. 4(a) shows the speed variation as a function of aquatic mortality $\bar{\mu}_2$ for different values of adult mortality $\bar{\mu}_1$. We observe that a great increase in aquatic mortality does not proportionally reduce the wave speed. One reason for this fact is that adult mosquitoes are the infected population, whereas mosquitoes in the aquatic phase are not. Another reason is that the aquatic population suffers neither diffusion nor advection, since we are neglecting

the transport regarding larvae and pupae. Then larvicide application against the aquatic form is not effective in controlling the front waves of the disease. Assuming that the curve at the top corresponds to the situation without adult control, we observe that the wave speed varies very slowly with aquatic mortality, from 21.53 km/year ($\bar{\mu}_2^{-1} = 18$ days) to 21.47 km/year ($\bar{\mu}_2^{-1} = 2$ days). All other curves correspond to the cases where insecticides are applied, which increase the mortality of adult mosquitoes. However, only when a high control is applied on the adult subpopulation (the bottom curve for $\bar{\mu}_1^{-1} = 6$ days), the wave speed varies a little with respect to the aquatic control, from 3.52 km/year ($\bar{\mu}_2^{-1} = 18$ days) to 1.71 km/year ($\bar{\mu}_2^{-1} = 2$ days). Similar results were obtained for the control of the front waves of mosquito invasion by larvicide [10], except that the wave speed of invasion decreasing as a function of aquatic mortality is more sensitive than the dengue wave speed.

Fig. 4(b) shows the speed variation as a function of mortality in the adult phase $\bar{\mu}_1$ for different values of mortality $\bar{\mu}_2$, in

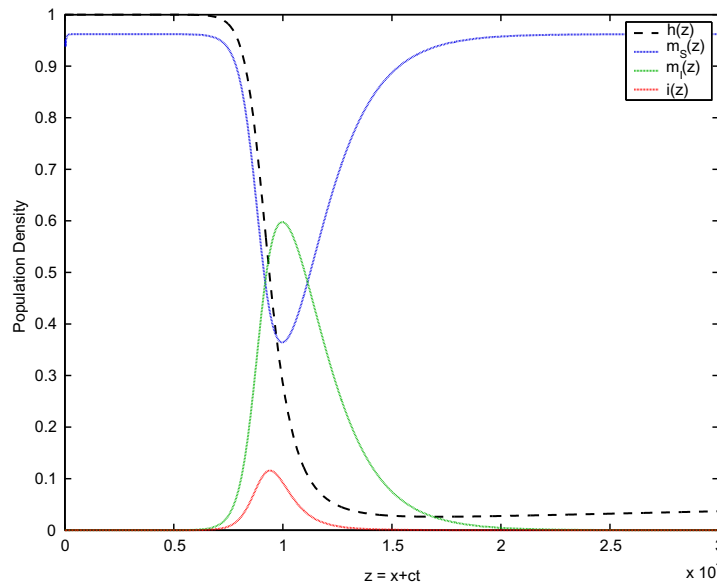


Fig. 2. Traveling waves for the system (21)–(27) using the non-dimensional parameters corresponding to those listed in Tables 1 and 2, setting $v = 0$, for infected and uninfected humans, and infected and uninfected mosquitoes. The first front wave of the disease can be observed.

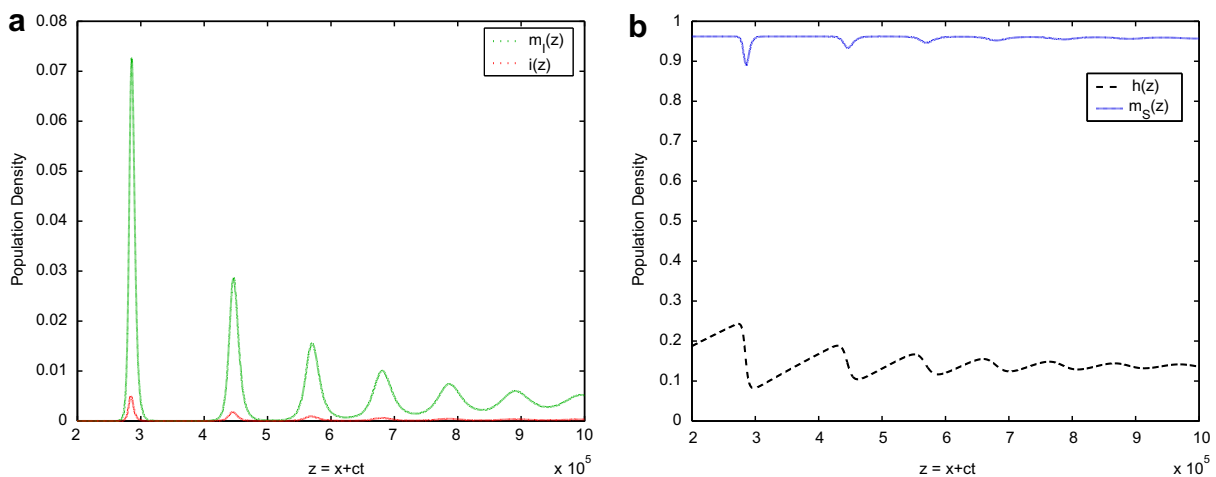


Fig. 3. Traveling waves for the system (21)–(27) using the non-dimensional parameters corresponding to those listed in Tables 1 and 2, setting $v = 0$, showing the damped oscillations of the disease for $200000 < z < 1000000$: (a) in the infected classes of both populations, and (b) in the susceptible classes of both populations.

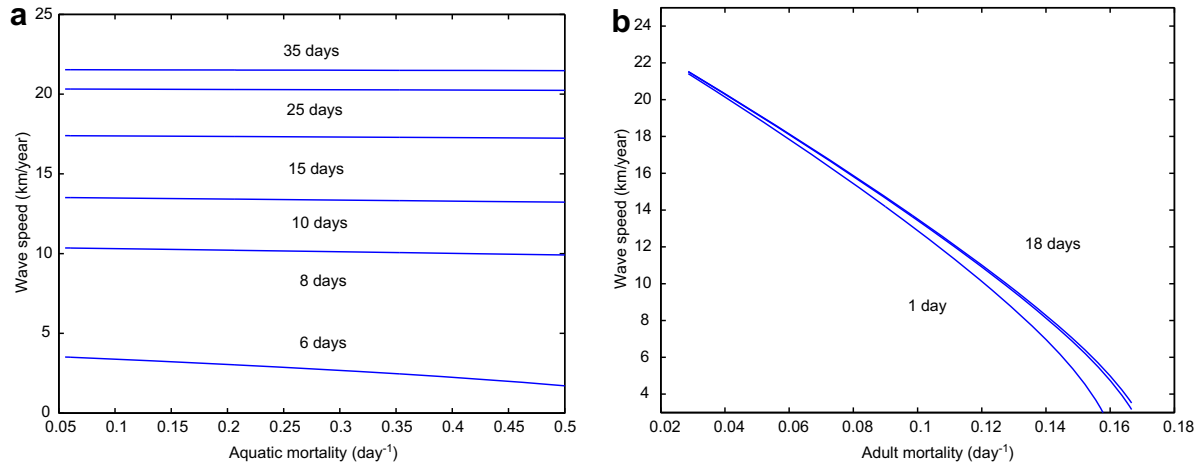


Fig. 4. (a) Variation of the wave speed as a function of aquatic mortality ($\bar{\mu}_2$) for four values of adult mortality, from top to bottom, we have $\bar{\mu}_1 = 0.0285714, 0.04, 0.0666667$ and 0.1666667 ($\bar{\mu}_1^{-1} = 35, 25, 15$ and 6 days). (b) Variation of the wave speed as a function of adult mortality ($\bar{\mu}_1$) for three values of aquatic mortality, from top to bottom, we have $\bar{\mu}_2 = 0.05555, 0.16666$ and 1 ($\bar{\mu}_2^{-1} = 18, 6$ and 1 days).

which case a considerable decrease in the wave speed is observed. An increase in the mortality of the aquatic phase does not affect significantly the wave speed for lower values of the adult mortality. It can be seen for the range $0.0285714 < \bar{\mu}_1 < 0.04$ ($25 \text{ days} < \bar{\mu}_1^{-1} < 35 \text{ days}$), where the curves practically coincide. For higher values of the adult mortality, $0.16 < \bar{\mu}_1 < 0.17$ ($5.88 \text{ days} < \bar{\mu}_1^{-1} < 6.25 \text{ days}$) the increase in $\bar{\mu}_2$ affects the wave speed differently (see that the curves do not coincide).

From Fig. 4(a) and (b), the use of larvicide to control the aquatic form is very limited on protecting a region from the onset of dengue, but, combined with the insecticide, the benefit of larvicide will be enhanced. On the other hand, the use of the insecticide in order to reduce the density of the winged form of mosquitoes strongly controls the dissemination of dengue disease. However, the question about the costs regarding the use of larvicide and insecticide is not taken into account, and neither are the effects of residual actions of larvicide and insecticide.

In Table 5 we present the theoretical front wave speed, using polynomial (29) and solving $P_1(\lambda_+) = 0$, for different temperatures. The model's parameters used are those given in Tables 1–3, with $v = 0$. In Table 3 we calculated the speed of biological invasion by mosquitoes for different temperatures and we matched one of them with the speed observed in the state of São Paulo. Taking into account the same set of values used to calculate the invasion by mosquitoes, now we calculate the front wave speed of dengue dissemination. The pair of values for $\bar{\beta}_1$ and $\bar{\beta}_2$ used in [2,3] was assigned for 30 °C, and for lower temperatures both values were decreased proportionally. The dimensional wave speeds are situated in the range [18.24–21.5] km/year, for [25 °C–30 °C]. For 15 °C, considering $\bar{\beta}_1 = 0.0014$ and $\bar{\beta}_2 = 0.0008$, the disease does not spread, even if we have the invasion of mosquitoes at a wave speed of 22 km/year.

Table 5
Dengue dissemination with parameters depending on temperature given in Tables 1 and 2, with $\bar{v} = 0$

Temp.	$\bar{\beta}_1$ (km ² /day)	$\bar{\beta}_2$ (km ² /day)	R_0	Disease speed (km/year)
15°–20°	0.0014–0.0021	0.0008–0.0015	0.49–1.95	0–13.43
20°–25°	0.0021–0.0028	0.0015–0.002	1.95–4.08	13.43–18.24
25°–30°	0.0028–0.0033	0.002–0.0025	4.08–7.29	18.24–21.53
30°	0.0033	0.0025	7.29	21.53

With respect to reproduction number R_0 , Chowell et al. [18] estimated R_0 using spatial data collected from Colima, Mexico, taking into account two types of model. The epidemic model with more realistic incubation and infectious periods estimated an average value of R_0 from 0.49 to 3.30, for average temperatures varying from 22.10 to 25.88 °C. Our model considering the temperatures from 20 to 25 °C predicts R_0 varying from 1.95 to 4.08. It must be considered that the whole population of the state of Colima is 488,028 and that the state of São Paulo has a population of approximately 45,000,000 individuals. For a value of $\bar{N}_0 = 100$ individuals per km², our model predicts R_0 from 1.30 to 2.72. This is in agreement with the fact that the basic reproduction numbers estimated in Brazil are higher than in other regions of the world (Massad et al. [19,20], Nishiura [21]).

4.3. The effect of advection on disease dissemination

In this section we study how advection increases the speed of disease dissemination. Polynomial $P_2(\lambda)$ has real roots because the discriminant is less than zero even for $v \neq 0$, then polynomial $P_1(\lambda)$ determines the wave speed. The equation to determine c_{\min} is the same as for the case $v = 0$, that is $P_1(\lambda_+) = 0$. In this case, the polynomial is not symmetric with respect to the y axis, as is observed in the case $v = 0$.

Calculating c from the equation $P_1(\lambda_+) = 0$, letting $v = -0.141421$, which describes the advection in the left direction, we obtain $c_{\min} = 0.282515$ for the corresponding non-dimensional parameters given in Tables 1 and 2. As a consequence of advection, the front wave speed is increased in the left direction, but lowered with respect to the right direction. In dimensional parameters, the leftward speed of disease dissemination is 0.1 km/day, approximately 36.5 km/year, higher than the speed 21.5 km/year obtained when advection is disregarded ($v = 0$).

In Fig. 5(a) we show that the speed increases with the advection in the left direction ($v < 0$). Independently of the transmission coefficient $\bar{\beta}_1$, the wave speed increases approximately 15 km/year when advection increases from 0 to 18.25 km/year. Observe that the advection coefficient increases the wave speed linearly for any values assumed by the other parameters.

In Fig. 5(b) we show the wave speed as a function of the transmission coefficient from human to vector $\bar{\beta}_1$, for the case without advection, $v = 0$, and with advection in the left direction, $\bar{v} = -18.25$ km/year ($v = -0.141421$). The wave speed increases more quickly for lower values of parameter $\bar{\beta}_1$. For higher values

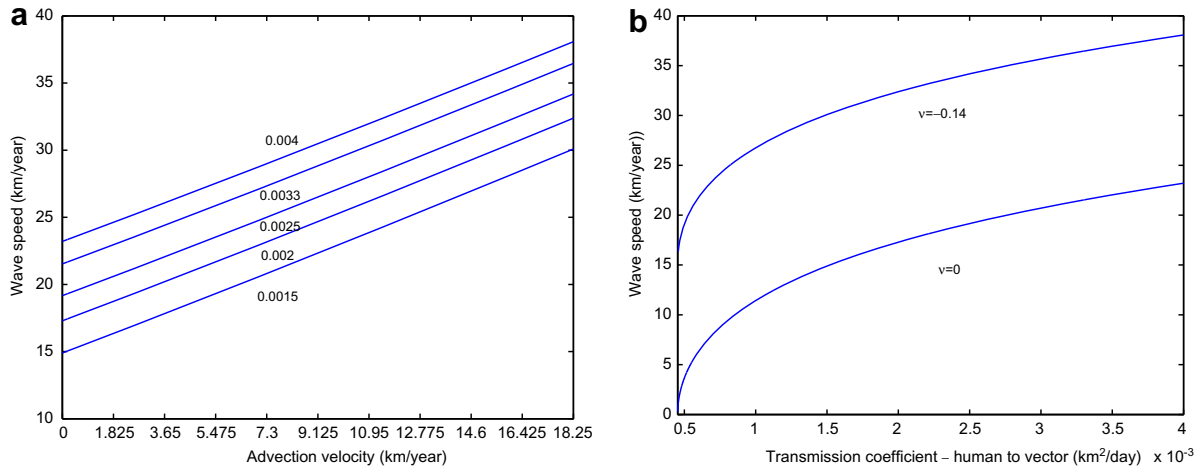


Fig. 5. (a) The wave speed variation as a function of the advection coefficient for different values of the transmission coefficient $\bar{\beta}_1 = 0.004, 0.0033, 0.0025, 0.002$ and 0.0015 . (b) The wave speed variation as a function of the transmission coefficient from human to vector $\bar{\beta}_1$, considering $\bar{v} = 0$ and 18.25 km/year in the left direction ($v = 0$ and -0.14).

of $\bar{\beta}_1$, for instance, on the interval $0.0025 < \bar{\beta}_1 < 0.004$, the wave speed varies slowly. Notice that, for $v = 0$, the waves velocity increases from 19.2 km/year to 23.2 km/year, much lower than the range of variation for lower $\bar{\beta}_1$. This fact is important because $\bar{\beta}_1$ is difficult to be estimate exactly, which depends on the biting rate and transmission probability. Considering the advection coefficient $\bar{v} = -18.25$ ($v = -0.14$) the wave speed increases approximately 15 km/year in comparison with the speed corresponding to $\bar{v} = 0$.

5. Human movements and dengue dissemination

We are interested in numerically studying the front wave of dengue disease by taking human movements into account. In the previous section, we dealt with the question of how the epidemic could propagate via mosquitoes in the neighborhood when one case of infected human appears in a region. In this section, we present the numerical results [22] when human movements are allowed.

First, let us simulate the dissemination of dengue disease without human movements. For this purpose, we solve numerically the system of PDE (10)–(14) with the initial conditions:

$$I(x, 0) = \begin{cases} I_0, & |x| \leq 1 \\ 0 & |x| > 1 \end{cases} \quad (30)$$

and

$$M_S(x, 0) = m^*, \quad A(x, 0) = a^*, \quad H(x, 0) = 1, \quad M_I(x, 0) = 0. \quad (31)$$

These conditions portray local introduction of I_0 infectious individuals in a region colonized by mosquitoes. For the boundaries, we apply null Neumann conditions:

$$\begin{aligned} \frac{\partial M_S}{\partial x}(\pm L, t) &= \frac{\partial M_I}{\partial x}(\pm L, t) = \frac{\partial A}{\partial x}(\pm L, t) = \frac{\partial H}{\partial x}(\pm L, t) \\ &= \frac{\partial I}{\partial x}(\pm L, t) = 0, \quad t > 0. \end{aligned} \quad (32)$$

In Fig. 6 we show the disease dissemination when one infected individual is introduced in a completely susceptible population. Fig. 6(a) and (b) show the dissemination of the first wave of epidemics at two times. The parameter values are those given in Tables 1 and 2. The front wave epidemic travels with speed $c = \frac{800-400}{4947.6-2552.4} = 0.167$, which agrees with the non-dimensional wave speed c_{\min} calculated with polynomial (29). The corresponding dimensional wave speed is 21.5 km/year (0.06 km/day).

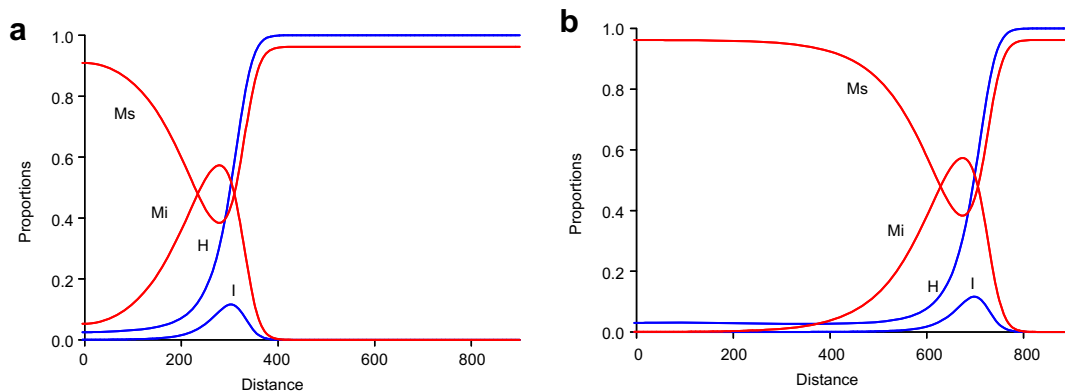


Fig. 6. Traveling wave solution of the PDE system (10)–(14) for the parameters listed in Tables 1 and 2, with $\bar{v} = 0$. The initial and boundary conditions are given by (30)–(32), with $I_0 = 1/150$, one individual infected. The solutions are plotted for times: (a) $t = 2552.4$, and (b) $t = 4947.6$. The wave propagates with speed $c_{\min} = 0.167$.

Now, we incorporate the human movements in the previous model, given by Eqs. (10), (12)–(14). The dimensional model is then given by:

$$\frac{\partial \overline{M}_S}{\partial t} = \overline{D}_M \frac{\partial^2 \overline{M}_S}{\partial x^2} - \overline{v} \frac{\partial \overline{M}_S}{\partial x} + \overline{\gamma} \overline{A} \left(1 - \frac{\overline{M}}{k_1} \right) - \overline{\mu}_1 \overline{M}_S - \overline{\beta}_1 \overline{M}_S \overline{I} \quad (33)$$

$$\frac{\partial \overline{M}_I}{\partial t} = \overline{D}_M \frac{\partial^2 \overline{M}_I}{\partial x^2} - \overline{v} \frac{\partial \overline{M}_I}{\partial x} - \overline{\mu}_1 \overline{M}_I + \overline{\beta}_1 \overline{M}_S \overline{I} \quad (34)$$

$$\frac{\partial \overline{A}}{\partial t} = r \left(1 - \frac{\overline{A}}{k_2} \right) \overline{M} - \overline{\mu}_2 \overline{A} - \overline{\gamma} \overline{A} \quad (35)$$

$$\frac{\partial \overline{H}}{\partial t} = \overline{D}_N \frac{\partial^2 \overline{H}}{\partial x^2} - \overline{\omega}_N \frac{\partial \overline{H}}{\partial x} + \overline{\mu}_H \overline{N} - \overline{\mu}_H \overline{H} - \overline{\beta}_2 \overline{H} \overline{M}_I \quad (36)$$

$$\frac{\partial \overline{I}}{\partial t} = \overline{D}_N \frac{\partial^2 \overline{I}}{\partial x^2} - \overline{\omega}_N \frac{\partial \overline{I}}{\partial x} + \overline{\beta}_2 \overline{H} \overline{M}_I - \overline{\sigma} \overline{I} - \overline{\mu}_H \overline{I} \quad (37)$$

$$\frac{\partial \overline{R}}{\partial t} = \overline{D}_N \frac{\partial^2 \overline{R}}{\partial x^2} - \overline{\omega}_N \frac{\partial \overline{R}}{\partial x} + \overline{\sigma} \overline{I} - \overline{\mu}_H \overline{R}. \quad (38)$$

As we are dealing with spatial movements of humans, the new parameters are the diffusion and advection of the human population, denoted by \overline{D}_N and $\overline{\omega}_N$, respectively. The human movements are really the source of long-distance transmission of dengue disease, and this system of equations is essential to study dengue transmission on a large scale.

Numerical simulations were performed using the non-dimensional system of equations corresponding to the dimensional system (33)–(38), using the non-dimensional parameters given in

(7)–(9) plus the new non-dimensional parameters $D^* = \frac{\overline{D}_N}{\overline{D}_M}$ and $\omega^* = \frac{\overline{\omega}_N}{r} \left(\frac{r}{\overline{D}_M} \right)^{1/2}$, which are the non-dimensional human diffusion and advection, respectively. The initial and boundary condition are those given by Eqs. (30)–(32). The parameter values are those given in Tables 1 and 2, and for the remaining parameters D^* and ω^* , the values are assigned according to the study.

In Fig. 7 we show the disease dissemination (the first wave of epidemic) when one infected individual is introduced in a completely susceptible population. The figure shows the simulation performed up to the time corresponding to Fig. 6(a), and the advection movement of humans was not considered ($\omega^* = 0$). In Fig. 7(a) the diffusive movement of the humans was left equal to that corresponding to the mosquito population, $D^* = 1$, that is, $\overline{D}_N = \overline{D}_M$. In this case, the wave speed is 25.8 km/year, which is 20% higher than that found in Fig. 6. When we let $D^* = 10$, that is, $\overline{D}_N = 10\overline{D}_M$, as shown in Fig. 7(b), the wave speed is 58.1 km/year, which is 170% higher than the speed without human movement. Notice that the increase in the diffusive movement in 10 times increased the rate of epidemic dissemination by less than 3 times.

Another interesting aspect of diffusion of humans is the enlargement of the front wave (compare, especially, Figs. 6(a) and 7(b)). The diffusive movement of humans does not have preferential direction, but occurs at random, for this reason, it does not only increase the rate of dengue dissemination, but it also sustains the disease for a longer period of time (expanding the region where the disease presents high incidence).

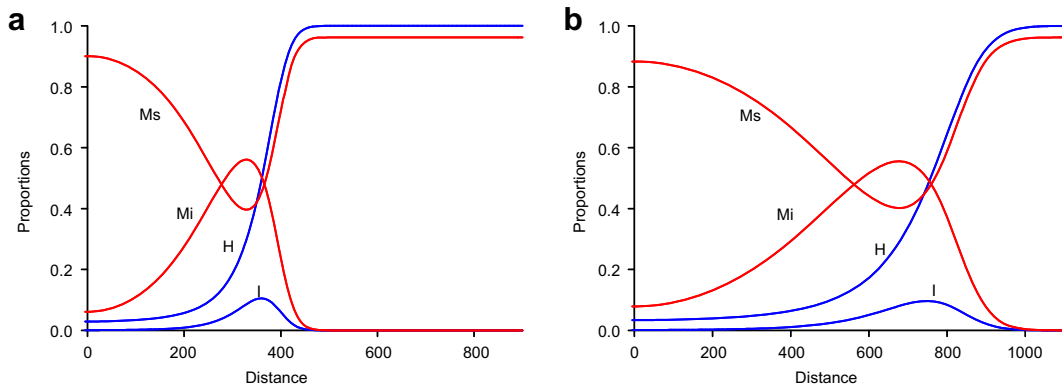


Fig. 7. Traveling wave solution of the PDE system (33)–(38) for the parameters listed in Tables 1 and 2, with $\overline{v} = 0$. The initial and boundary conditions are given by (30)–(32), with $I_0 = 1/150$, one individual infected, plotted at time $t = 2552.4$. In this case we considered, for human diffusion, (a) $\overline{D}_N = \overline{D}_M$, and (b) $\overline{D}_N = 10\overline{D}_M$.

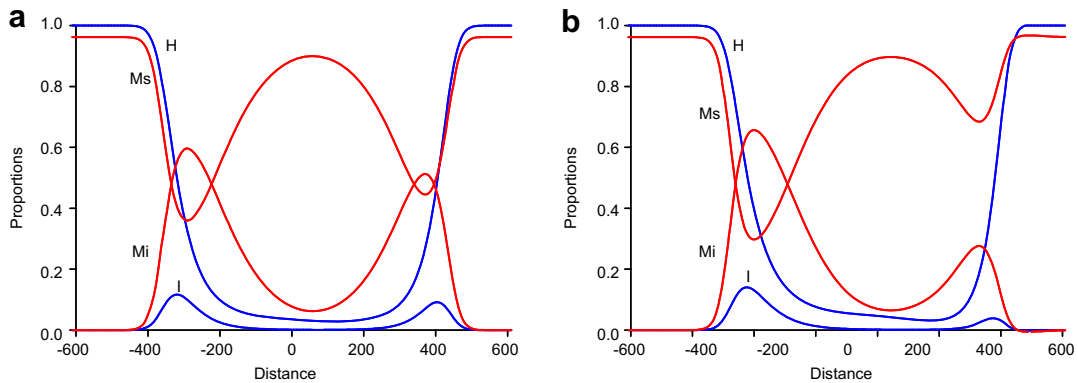


Fig. 8. Traveling wave solution of the PDE system (33)–(38) for the parameters listed in Tables 1 and 2, with $\overline{v} = 0$. The initial and boundary conditions are (30)–(32), with $I_0 = 1/150$, one individual infected, plotted at time $t = 2552.4$. In this case we considered, for human diffusion, $\overline{D}_N = \overline{D}_M$ and different advection values: (a) $\omega^* = 0.05$, and (b) $\omega^* = 0.2$.

In Fig. 8 we show the disease dissemination (the first wave of the epidemic) when one infected individual is introduced in a completely susceptible population. The figure shows the simulation performed up to the time corresponding to Fig. 6(a), and the diffusive movement of humans was set at $D^* = 1$, that is, $\bar{D}_N = \bar{D}_M$. In Fig. 8(a) the advection movement of humans was set at $\omega^* = 0.05$. In this case, the wave speed is 28.4 km/year, which is 10% higher than that found in Fig. 7(a). When we let $\omega^* = 0.2$, as shown in Fig. 8(b), the wave speed is 37.4 km/year, which is 45% higher than the speed found in Fig. 7(a). Notice that a fourfold increase in the advection movement speeded up the rate of the epidemic dissemination by less than 1.5 times. Note that the advection movement ($\omega^* = 0.2$) is 5 times smaller than the diffusive movement of humans; but even so, it significantly increased the wave speed.

If the advection movement is not considered, the epidemic wave propagates with the same speed in both directions on the x -axis (Figs. 6 and 7 present only positive values of x). The advection movement, in the positive direction of x -axis, changed the epidemic wave propagation, increasing the wave speed with respect to the positive x -axis, and decreasing it in the opposite direction (Fig. 8 presents both directions of the x -axis). In the long-term propagation of dengue, the major contribution to the quick spread of dengue disease is due to human movements. In a further work, we analyze dengue propagation in more detail, including human movements.

Another interesting aspect regarding the movement of humans is the shrinking of the front wave in the advective direction (compare, especially, Figs. 7(a) and 8(b)). The advective movement of humans draws infectious humans in a preferential direction, for this reason, it does not only increase the speed of dengue propagation, but it also shortens disease duration (by shortening the region where the disease is endemic and decreasing its incidence). However, no difference was observed in the opposite direction of advection.

6. Conclusion

In this work, we developed a simple model to assess the geographical spread of dengue disease. We assumed that only adult mosquitoes disseminate through dispersion and advection. From the model, a threshold value is determined as a function of the model's parameters:

$$R_0 = \frac{\beta_1 \beta_2 m^*}{\mu_1(\mu_H + \sigma)}.$$

This is the basic reproductive number, which determines the existence of the endemic status. If R_0 is less than one the disease fades out. Otherwise, if R_0 is greater than one, the mosquito and human populations will approach the endemic status.

The existence of the mosquito population, m^* , in the numerator, is a necessary condition for the existence of the disease, as we expected. The condition for the existence of the mosquito population is the same as in [10], that is,

$$Q_0 = \frac{\gamma}{\mu_1(\gamma + \mu_2)}.$$

If Q_0 is greater than one the mosquito population exists. Otherwise, if Q_0 is less than one, the mosquito population does not exist and, hence, the disease does not exist.

The analysis of the model to determine the front wave speed of colonization by mosquitoes was performed, and also the dissemination rate of dengue disease was determined. An important result

is the implicit equation to obtain the minimum traveling wave speed, given by polynomial (29):

$$P_1(\lambda_+) = 0.$$

The basic offspring number Q_0 and the basic reproduction number R_0 determine this speed.

In the study of biological invasion by mosquitoes, we fitted our model to the invasion and colonization by *A. aegypti* in the state of São Paulo. The minimum traveling wave speed obtained from the model was compared to the estimated invasion and colonization by mosquitoes in the state of São Paulo. We can obtain a good estimation if we take into account entomological parameters at 20 °C. Similarly, we determined the wave speed of dengue dissemination in an area previously colonized by *A. aegypti*, allowing movements only to the mosquito population. In addition, we numerically calculated the wave speed by allowing movements to humans, too.

The wave speed is a function of the model's parameters. This fact permitted the assessment of control strategies. The results allowed us to evaluate strategies in order to attain the eradication of dengue transmission by decreasing the dissemination rate to zero. The variation of the wave speed as a function of mortality rates, aquatic and adult phases, was shown in Fig. 4(a) and (b). The decrease in the wave speed as a function of aquatic mortality is negligible. Then, larvicide application against the aquatic form is not effective to break the front waves of the disease. On the other hand, with respect to adult mortality, we can see a considerable decrease in the wave speed.

Our aim in this paper was to determine the dissemination of dengue by only the diffusive movement of adult mosquitoes. In fact, the long-distance movement of the human population is the major contributor to the quick dissemination of dengue disease across geographical regions. For instance, the state of São Paulo registered the first dengue outbreak in Araçatuba and neighboring regions in 1987. However, the dengue strongly re-emerged in Ribeirão Preto and neighboring towns 3 years later, and then in 1991, dengue disease was recorded in regions farther than 150 km from Ribeirão Preto [9]. This feature of dengue dissemination leads us to include human movements, which considerably increase the dissemination rate [14], as a consequence of the movements of the infected population. This fact is in agreement with other results [6], where the estimated dissemination rate was 114–209 km/month.

Finally, this model sheds some light upon the role of mosquito movements in local dengue distribution [7] and human movements in long-distance dissemination [6]. The diffusive and advective movements of mosquitoes increase the rate of dengue dissemination, but not so intensively. Nevertheless, human movements contribute much more to dengue dissemination, since advection influences disease dissemination much more than does diffusion. Additionally, the advective movement in a preferential direction generated a very sharp front wave (in the advective direction) than did the diffusive movement. However, if the diffusive movement is high and also more important than the advective one, we expect to observe a quick rate of dengue dissemination associated with a spatially broad distribution of dengue incidence.

Acknowledgments

We thank Professor Jones Colombo and Professor Jose Luiz Boldrini for the computational suggestions. We also thank the comments and suggestions provided by anonymous referees, which contributed to improving this paper.

Appendix A. Stability analysis of the equilibrium points

We present the stability of the equilibrium points E_0 and E_1 .

A.1. Proof of Theorem 3.1

The characteristic polynomial of the Jacobian matrix corresponding to the system (15)–(19) evaluated at point E_0 is:

$$p_1(\lambda) = -(\mu_1 + \lambda)(\mu_H + \lambda)(\mu_H + \sigma + \lambda)[\mu_1(\gamma + \mu_2)(Q_0 - 1) + (\gamma + \mu_1 + \mu_2)\lambda + \lambda^2].$$

The eigenvalues are: $\lambda_1 = -\mu_1$, $\lambda_2 = -\mu_H$, $\lambda_3 = -(\mu_H + \sigma)$ and the roots of the polynomial:

$$p_2(\lambda) = \mu_1(\gamma + \mu_2)(Q_0 - 1) + (\gamma + \mu_1 + \mu_2)\lambda + \lambda^2.$$

Hence E_0 is stable if the coefficients of the polynomial $p_2(\lambda)$ are positive, which are satisfied when $Q_0 < 1$. Conversely, if $Q_0 > 1$, then $p_2(0) < 0$. So $p_2(\lambda)$ has a positive real root.

A.2. Proof of Theorem 3.2

The characteristic polynomial of the Jacobian matrix corresponding to the system (15)–(19) evaluated at point E_1 is:

$$p_3(\lambda) = -(\mu_1 + \lambda)p_4(\lambda)p_5(\lambda).$$

The eigenvalues are: $\lambda_1 = -\mu_1$, and the roots of the polynomials:

$$p_4(\lambda) = \left[\mu_1(\gamma + \mu_2)(Q_0 - 1) + \left(\frac{\gamma + k\mu_1}{\gamma + k + \mu_2} + \frac{\gamma + k + \mu_2}{\gamma + k\mu_1} \right) \lambda + \lambda^2 \right],$$

and

$$p_5(\lambda) = [\mu_1(\mu_H + \sigma)(1 - R_0) + (\mu_1 + \mu_H + \mu_\sigma)\lambda + \lambda^2].$$

Hence E_1 is stable if the coefficients of the polynomials $p_4(\lambda)$ and $p_5(\lambda)$ are positive, which are satisfied when $Q_0 > 1$ and $R_0 < 1$. Conversely, if $Q_0 < 1$, then $p_4(0) < 0$. So $p_4(\lambda)$ has a positive real root. If $R_0 > 1$, the same argument provides that $p_5(\lambda)$ has a positive real root.

Appendix B. Traveling wave solutions

We present details regarding the traveling wave speed.

B.1. Traveling wave connecting \widehat{E}_0 with \widehat{E}_1

We seek traveling wave solutions in the three-dimensional submanifold

$$\widehat{M} = \{(m_s, u, m_i, v, a, h, i) : m_i = 0, v = 0, h = 1, i = 0\},$$

because we are considering the situation where the disease cannot be sustained ($R_0 < 1$).

We are dealing with a biological system, then the trajectories must not oscillate around the zero components, which are population densities. Then the eigenvalues must be real.

The corresponding equilibrium point to E_1 is $\widehat{E}_1 = (m^*, 0, 0, 0, a^*, 1, 0)$, which does not have zeros for the densities in this submanifold. Then we must only analyze the eigenvalues at the equilibrium point corresponding to E_0 , i.e., $\widehat{E}_0 = (0, 0, 0, 0, 0, 1, 0)$, where the densities of mosquitoes in adult and aquatic phases are zero.

The first four eigenvalues for the equilibrium point \widehat{E}_0 are real:

$$\lambda_1 = -\frac{\mu_H}{c}, \quad \lambda_2 = -\frac{\mu_H + \sigma}{c},$$

and

$$\lambda_{3,4} = \frac{1}{2} \left[c + v \pm \sqrt{(c + v)^2 + 4\mu_1} \right].$$

Then we must determine when the polynomial $P(\lambda)$, given by:

$$P(\lambda) = \lambda^3 + \left[-(c + v) + \frac{(\mu_2 + \gamma)}{c} \right] \lambda^2 - \left[\mu_1 + (c + v) \frac{(\mu_2 + \gamma)}{c} \right] \lambda + \frac{\mu_1(\gamma + \mu_2)(Q_0 - 1)}{c},$$

has all roots with real values. The polynomial $P(\lambda)$ has the same shape as the polynomial $P_1(\lambda)$. We know that $Q(0) > 0$, since we are taking into account the case $Q_0 > 1$; additionally, we have:

$$\lim_{\lambda \rightarrow \pm\infty} P(\lambda) = \pm\infty$$

and

$$\left. \frac{dP(\lambda)}{d\lambda} \right|_{\lambda=0} = - \left(\mu_1 + (c + v) \frac{(\mu_2 + \gamma)}{c} \right) < 0,$$

then the polynomial has always a negative real root. With respect to the two remaining roots, we first determine the extrema λ_{\pm} of this polynomial (they must satisfy $\frac{d}{d\lambda} P(\lambda) = 0$), which are given by

$$\lambda_{\pm} = \frac{1}{3} \left\{ - \left[-(c + v) + \frac{(\mu_2 + \gamma)}{c} \right] \pm \sqrt{\left[-(c + v) + \frac{(\mu_2 + \gamma)}{c} \right]^2 + 3 \left[\mu_1 + (c + v) \frac{(\mu_2 + \gamma)}{c} \right]} \right\}.$$

If we impose, to the local minimum $\lambda_{+} > 0$, that $P(\lambda_{+}) \leq 0$, i.e., $P(\lambda_{+})$ is at most zero, then the roots are real values. From this equation we obtain the speed of invasion of mosquitoes by calculating the value of c that satisfies $P(\lambda_{+}) = 0$.

Considering $c \geq c_{\min}$, we have three real roots for the polynomial $P(\lambda)$, say $z_i(c)$, $i = 1, 2, 3$. Linearizing the system about the steady state $(0,0,0,0,0,1,0)$, we obtain the eigensolutions corresponding to the submanifold \widehat{M} :

$$\begin{pmatrix} m_s \\ u \\ m_i \\ v \\ a \\ h \\ i \end{pmatrix} = b_i \exp[z_i(c)z],$$

where

$$b_i^T = ((1/k)(\gamma + \mu_2 + cz_i(c)), (1/k)z_i(c), 0, 0, 1, 0, 0),$$

i.e., the trajectories remain in the three-dimensional manifold \widehat{M} , and the analysis is the same as in [10]. This trajectory means that the mosquitoes are able to invade and colonize regions that are free of them, assuming that human population is present.

*B.2. Traveling wave connecting \widehat{E}_1 with \widehat{E}^**

In this case, we search for wave solutions in the manifold $(m_s, u, m_i, v, a, h, i)$. The corresponding equilibrium point to E^* is $\widehat{E}^* = (M_s^*, 0, M_i^*, 0, A^*, H^*, I^*)$, which does not have zero components corresponding to the densities. Then we must study the oscillations around the equilibrium point $\widehat{E}_1 = (m^*, 0, 0, 0, a^*, 1, 0)$, considering that this point has zero components with respect to the

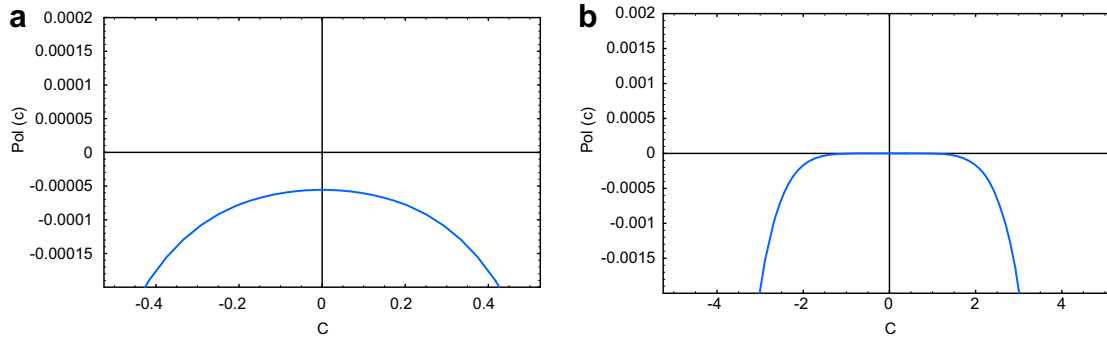


Fig. 9. (a) Graph of the polynomial $pol(c)$ for the non-dimensional parameters corresponding to those listed in Table 1. (b) Graph of the polynomial $pol(c)$ for the non-dimensional parameters corresponding to those listed in Table 1, setting $\gamma_c = 0.0000159186$, in which case we have $a^* = 0$ and $m^* = 0$. The maximum is reached in the origin of this critical value.

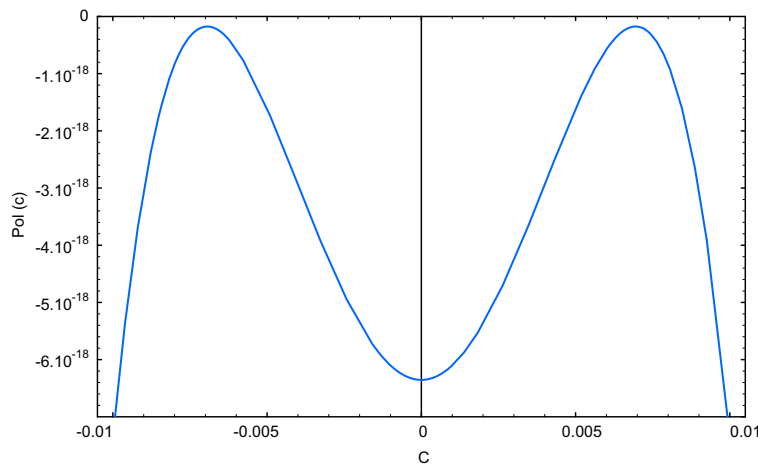


Fig. 10. Graph of the polynomial $pol(c)$ for the non-dimensional parameters corresponding to those listed in Table 1, setting $\mu_2 = 10^{-20}$ and $\gamma = 10^{-6}$. For parameters $\mu_2 \ll 1$ and $\gamma \ll 1$, the coefficient a_2 becomes positive, but the discriminant remains less than zero.

infective classes. To avoid oscillations around this point, we must not have complex eigenvalues. The eigenvalues are:

$$\lambda_1 = -\frac{\mu_H}{c},$$

plus the roots of the two third-degree polynomials:

$$P_1(\lambda) = \lambda^3 + \left[-(c + v) + \frac{(\mu_H + \sigma)}{c} \right] \lambda^2 - \left[\mu_1 + (c + v) \frac{(\mu_H + \sigma)}{c} \right] \lambda + \frac{\mu_1(\mu_H + \sigma)(R_0 - 1)}{c}$$

and

$$P_2(\lambda) = \lambda^3 + \left[-(c + v) + \frac{\gamma + \mu_2 + k\mu_1^*}{c} \right] \lambda^2 + \left[-(c + v) \frac{(\gamma + k\mu_1^* + \mu_2)}{c} - \left(\frac{a^*\gamma + k\mu_1}{k} \right) \right] \lambda - \frac{\mu_1(\gamma + \mu_2)(Q_0 - 1)}{c}.$$

The polynomial $P_2(\lambda)$ is structured in terms of the parameters regarding the mosquito population only and comprises neither the human population parameters nor the infection parameters. The polynomial $P_1(\lambda)$ determines the wave speed, because the polynomial $P_2(\lambda)$ has all roots with real values. An idea of the proof is the following: We apply Cardan's formula [23] and write the discriminant of $P_2(\lambda)$ as a new polynomial in c . The discriminant has the form:

$$dis(c) = pol(c)/c^4,$$

with $pol(c) = a_6c^6 + a_4c^4 + a_2c^2 + a_0$, where the coefficients a_i , for $i = 0, 2, 4$ and 6 , depend on the parameters γ, μ_1, μ_2 and k . For the corresponding values of the parameters of *A. aegypti* given in Table 1, setting $v = 0$, all the coefficients a_i are negative, which implies that the discriminant is less than zero, and the polynomial has only real roots (see Fig. 9). In this case, the non-dimensional value of γ is 0.02.

When the value of the transition parameter γ decreases to a critical value, given by $\gamma_c = 0.0000159186$, in which case the mosquito population does not exist ($a^* = 0$ and $m^* = 0$), the maximum of the polynomial $pol(c)$ increases, but always assumes values less than zero. Only in this critical situation the maximum of $pol(c)$ is zero in the origin (see Fig. 9). This is a consequence of condition (20) being equal to zero ($Q_0 = 1$) and the independent coefficient a_0 ,

$$a_0 = \frac{[(1 - Q_0)]4\gamma^3(\gamma + k + \mu)^3}{27(\gamma + k\mu_1)^3},$$

is also zero.

If we allow the mortality rate of aquatic phase to have small values ($\mu_2 \ll 1$), together with small transition coefficient ($\gamma \ll 1$), we have positive coefficient $a_2, a_2 > 0$, but the discriminant is less than zero, and then polynomial $P_2(\lambda)$ has all roots with real values, see Fig. 10. This case does not have biological significance.

References

- [1] http://www.cve.saude.sp.gov.br/hm/zoo/dengue_inf2103.htm (September 27, 2007).
- [2] L. Esteva, C. Vargas, Analysis of a dengue transmission model, *Math. Biosci.* 150 (1998) 131.
- [3] L. Esteva, C. Vargas, Influence of vertical and mechanical transmission on the dynamic of dengue disease, *Math. Biosci.* 167 (2000) 51.
- [4] L. Esteva, C. Vargas, Coexistence of different serotypes of dengue virus, *J. Math. Biol.* 46 (2003) 31.
- [5] M. Derouich, A. Boutayeb, Dengue fever: mathematical modelling and computer simulation, *Appl. Math. Comput.* 177 (2006) 528.
- [6] D.A.T. Cummings, R.A. Irizarry, N.E. Huang, T.P. Endy, A. Nisalak, K. Ungchusak, D.S. Burke, Travelling waves in the occurrence of dengue haemorrhagic fever in Thailand, *Nature* 427 (2004) 344.
- [7] A. Tran, M. Raffy, On the dynamic of dengue epidemics from large-scale information, *Theoret. Population Biol.* 69 (2006) 3.
- [8] C. Moreno Glasser, Estudo da infestação do estado de São Paulo por *Aedes aegypti* e *Aedes Albopictus*, Dissertação de mestrado, Faculdade de Saúde Pública da Universidade de São Paulo, 1997.
- [9] http://www.cve.saude.sp.gov.br/hm/zoo/den_dir06.htm (September 27, 2007).
- [10] L.T. Takahashi, N.A. Maidana, W.C. Ferreira Jr., P. Pulino, H.M. Yang, Mathematical models for the *Aedes aegypti* dispersal dynamics: traveling waves by wing and wind, *Bull. Math. Biol.* 67 (2005) 509.
- [11] H.M. Yang, M.L.G. Macoris, K.C. Galvani, M.T.M. Andrighetti, Dinamica de transmissão de dengue com dados entomológicos temperatura-dependentes, *Tema-Tend. Mat. Apl. Comput.* 8 (1) (2007) 159.
- [12] L.C. Harrington, T.W. Scott, K. Lerdthusnee, R.C. Coleman, A. Costero, G.G. Clark, J.J. Jones, S. Kitthawee, P.K. Yamong, R. Sithiprasasna, J.D. Edman, Dispersal of the dengue vector *Aedes aegypti* within and between rural communities, *Am. J. Trop. Med. Hyg.* 72 (2) (2005) 209.
- [13] R. Veronesi, Doenças infecciosas e parasitárias, Guanabara Koogan SA, 1991.
- [14] J.D. Murray, *Mathematical Biology*, Springer, Berlin, 2002.
- [15] J.D. Murray, F.R.S. Stanley, D.L. Brown, On the spatial spread of rabies among foxes, *Proc. R. Soc. Lond.* B229 (1986) 111.
- [16] B. Sandstede, Stability of traveling waves, in: B. Fiedler (Ed.), *Handbook of Dynamical System II*, Elsevier, Amsterdam, 2002, p. 983.
- [17] A.I. Volpert, V.A. Volpert, *Traveling Wave Solutions of Parabolic System*, American Mathematical Society, Providence, RI, 1994.
- [18] G. Chowell, P. Diaz-Dueñas, J.C. Miller, A. Alcazar-Velazco, J.M. Hyman, P.W. Fenimore, C. Castillo-Chavez, Estimation of the reproduction number of dengue fever from spatial epidemic data, *Mathematical Bioscience* 208 (2007) 571.
- [19] E. Massad, F.A. Coutinho, M.N. Burattini, L.F. Lopez, The risk of yellow fever in a dengue-infested area, *Trans. R Soc. Trop. Med. Hyg.* 95 (4) (2001) 370.
- [20] E. Massad, M.N. Burattini, F.A. Coutinho, L.F. Lopez, Dengue and the risk of urban yellow fever reintroduction in Sao Paulo State, Brazil. *Rev. Saude Publica* 37 (4) (2003) 477.
- [21] H. Nishiura, Mathematical and statistical analyses of the spread of dengue, *Dengue Bull.* 30 (2007) 51.
- [22] FlexPDE 5.0 copyright 2005 PDE solution inc.
- [23] J. Rotman, *Galois Theory*, Springer, New York, 1990.